Research article Available online www.ijsrr.org ISSN: 2279–0543

International Journal of Scientific Research and Reviews

Synthesis and Structural Behavior of Co Doped $Ba(Ti_{0.85}Sn_{0.15})O_3$

Singh Sindhu

Department of Physics and Electronics, Dr. Rammanohar Lohia Avadh University, Faizabad-224001, India
E-Mail: sindhusingh@rmlau.ac.in

ABSTRACT

Effect of cobalt (Co) substitution on structural behavior of $Ba(Ti_{0.85}Sn_{0.15})O_3$ has been studied. Compositions with x = 0.01 and 0.03 in the system $Ba(Ti_{0.85-x}Co_xSn_{0.15})O_3$ were prepared by solid state ceramic method. X-ray Diffraction studies confirmed the formation of cubic single phase solid solutions at room temperature. Crystallite size determined by X-ray line broadening and by Scanning Electron Micrographs show good agreement.

KEY WORDS: High Dielectric Constant, Diffuse Phase Transition, Scanning Electron Micrograph, X-ray Diffraction, Solid State Ceramic Route

***Corresponding Author:**

Sindhu Singh

Department of Physics and Electronics,

Dr. Rammanohar Lohia Avadh University, Faizabad-224001,

India, E-Mail: sindhusingh@rmlau.ac.in

INTRODUCTION

Ferroelectric relaxors have many potential applications as materials having high dielectric constant, ε_0, as hysteresis free actuators and high performance sensors etc.[1, 2]. Relaxor ferroelectrics exhibit a diffuse i.e. a broad peak at a particular temperature T_m in their ε_0 vs T plots. Its position shifts to higher temperature with increasing frequency of measurement. Pronounced variation in the value of ε_0 is observed around peak maxima T_m. Lead-based perovskite oxides having more than one type of ions occupying the equivalent six co-ordinated crystallographic sites are well known for exhibiting relaxor properties[3]. But these oxides are toxic in nature. Therefore at present there is lot of interest in developing lead free compositions having lower temperature coefficient of dielectric constant near the peak temperature, which should be preferably around ambient conditions for above mentioned applications. Barium tin titanate $Ba(Ti_{1-x}Sn_x)O_3$ is one such potential system which has been studied extensively[4-7]. Diffuse Phase Transition (DPT) behavior is different from both the normal ferroelectrics and relaxor ferroelectrics[8]. It is characterized by a broad maxima in ε_0 vs T plots whose position is independent of frequency of measurement.

Nb_2O_5, CoO, NiO, MnO and some rare earth oxides have been doped in $BaTiO_3$ to improve its temperature stability[9, 10]. These additives broaden/diffuse the sharp dielectric constant peak at 120^0C observed in $BaTiO_3$[11-15]. Dopant like CoO inhibits the grain growth during sintering and form a so called “core-shell" structure inside the grain to limit the movement of domain walls[16]. Keeping in mind the significant change in the properties of $BaTiO_3$ due to substitution of Sn and Co independently, it was considered worthwhile to study the effect of their codoping on Ti site on the structural behavior of $BaTiO_3$. For this purpose, the most technologically potential composition, $Ba(Ti_{0.85}Sn_{0.15})O_3$, having highest dielectric constant in the system $Ba(Ti_{1-x}Sn_x)O_3$ is chosen[18-19]. Results of these investigations have been reported in this paper.

EXPERIMENTAL PROCEDURE:

Samples were prepared by solid state ceramic method using $BaCO_3$ (Thomas Baker, India), TiO_2 (Reidel Chemicals, India), SnO_2 (Himedia, India) having purity > 99.5% and cobalt oxalate (Himedia, India) with purity > 99.99% as raw materials. Appropriate amounts of these chemicals were mixed in a ball mill for six hours using agate jars & agate grinding media and acetone as a mixing medium. For calcination the mixed powders were dried, ground for half an hour and then kept at 1523K for 6 hours in a platinum crucible. Calcined powders were ground and mixed uniformly with a few drops of 2% solution of polyvinyl alcohol as a binder. Cylindrical pellets

having thickness in the range 1-2 mm and diameter 12 mm were prepared by pressing the uniformly mixed powder in a hydraulic press under an optimum load of 65 kN. These pellets were kept on a platinum foil and heated at a rate of 2K/min upto 773 K and kept at this temperature for about two hours to burn off the binder completely. Thereafter the temperature was raised at a rate of 4K/min to the sintering temperature 1623 K. At this temperature, the samples were sintered for 6 hours, where both sintering as well as solid state reaction amongst various constituents take place.

Powder X-ray diffraction patterns were recorded by X-ray Diffractometer (Rigaku Rotaex RTP 300) employing CuK_1 radiation with a Ni filter using grounded powder of sintered pellets. Archimedes principle was used for determination of density of the sintered pellets.

For Scanning Electron Micrograph (SEM) sintered pellets of each composition were polished using emery papers of grade 0/0, 1/0, 2/0, 3/0, 4/0 and 5/0 successively. One of the polished pellet is further polished on a velvet cloth with diamond paste of the order of 1μm and 1/4μm. For microstructural studied the pellets were cleaned using distilled water followed by methanol. Then they were chemically etched. Chemically etched pellets were coated with gold using "Hummer" sputtering coating unit and micrographs were taken using "Hitachi-S-4700, Field Emission SEM (FESEM)"

RESULTS AND DISCUSSION

(a) Crystal Structure and Density

Attempts were made to prepare compositions with x = 0.00, 0.01, 0.03 and 0.05, abbreviated as BTS, BTCS1, BTCS3 and BTCS5 in the system $Ba(Ti_{0.85-x}Co_xSn_{0.15})O_3$. Powder XRD patterns of the samples show that compositions with x = 0.00, 0.01 and 0.03 are single phase solid solution (Figure 1). XRD pattern of the composition with x = 0.05 contains lines of constituent oxides. Solid solution forms for $x \leq 0.03$ among the studied compositions. XRD data of the compositions with x = 0.00, 0.01 and 0.03 could be indexed on the basis of a cubic unit cell. Powder XRD data of these compositions were compared with JCPDS Card 31-0174. Lattice parameters were calculated by means of the UNITCELL-97 program[20-21]. Lattice parameter for all the three compositions is given in Table 1.

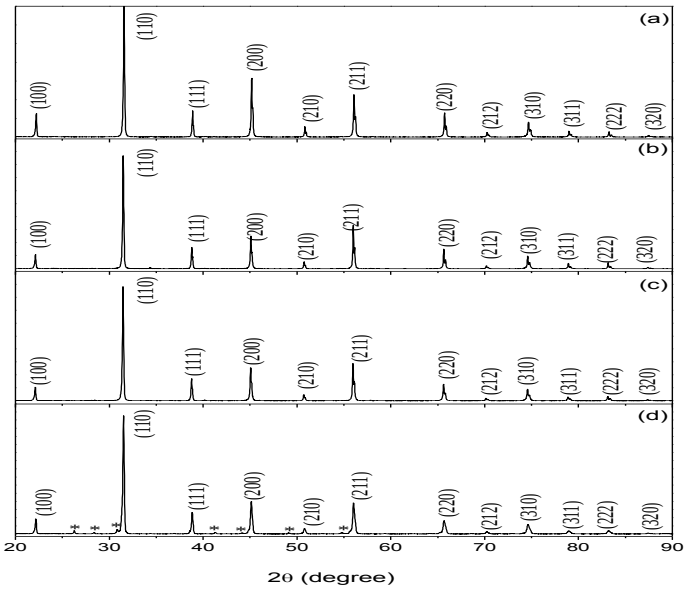

Figure No.1: XRD patterns for various compositions with x (a) 0.00 (b) 0.01 (c) 0.03 and (d) 0.05 in the system $BaTi_{0.85-x}Sn_{0.15}Co_xO_3$ prepared by solid state ceramic route

Table1: Composition, lattice parameter, theoretical density, experimental density and percentage porosity for samples in the system $Ba(Ti_{0.85-x}Co_xSn_{0.15})O_3$

Composition	Lattice Parameter(Å)	Theoretical Density (gm/cm^3)	Experimental Density(gm/cm^3)	% Porosity
BTS	4.0197	6.23	5.53	11.0
BTCS1	4.0206	6.24	5.79	7.0
BTCS3	4.0219	6.23	5.61	10.0

Lattice parameter is slightly larger for cobalt doped samples than that of BTS. This indirectly shows that cobalt ions exist mostly in Co^{2+} state. (Ionic radius of Co^{2+} and Ti^{4+} are (0.735 Å) and (0.605 Å) respectively[22]. Presence of cobalt in +3 oxidation state in slight amount cannot be ruled out. Oxidation state of Co needs to be confirmed by using XPS which is planned to do in near future. Theoretical density determined from the unit cell volume and molecular weight of the compound. Theoretical density, experimental density and percentage porosity are given in Table 1. Porosity present in the three compositions is around 10%. Densification of samples improves with increasing

Co doping i.e. x. On doping Co^{2+}/Co^{3+} at Ti^{4+} site, oxygen vacancies are produced according to the reaction

$$BaO + CoO \xrightarrow{TiO_2} Ba_{Ba} + Co''_{Ti} + 2O_o + V_o^{\bullet\bullet} \quad (1)$$

Or

$$Co_2O_3 + 2BaO \xrightarrow{2TiO_2} 2Ba_{Ba} + 2Co'_{(Ti,Sn)} + 5O_O + V_O^{\bullet\bullet} \quad (2)$$

where all the species are written in accordance with Kröger Vink notation of defects[23]. Presence of $V_O^{\bullet\bullet}$ increases diffusion of O^{2-} which seems to promote densification.

Crystallite size for the powder samples was determined from the X-ray line broadening using Scherrer's formula

$$W = \frac{0.9\lambda}{dCos\theta} \quad (3)$$

Where W is the width at half maximum intensity of a Bragg reflection excluding instrumental broadening, λ is the wavelength of the X-ray radiation and θ is the Bragg angle. W for this sample is taken for strongest Bragg's peak corresponding to 2θ =31.45 and 31.44 for BTCS1 and BTCS3 respectively. The average particle size was found to be ~ 570 and 550 nm for BTCS1 and BTCS3 respectively.

(b) Microstructure:

Scanning Electron Micrograph for the samples BTCS1 and BTCS3 at different magnifications are shown in figures respectively. It is noted from the figures that dense microstructure is obtained. Upto a magnification in the range 6-10 k pores, grains with size ranging from 2-5 μm and distinct boundaries are observed. When the magnification of the microscope is increased above 20k subgrain microstructure within bigger grains is observed. Each grain is composed of large number of smaller grains(subgrains). Average subgrain size determined by linear intercept method from scanning electron micrograph has been found to be in the range 220-310 nm for BTCS1 and 100-120 nm for BTCS3 respectively. This shows reasonably good agreement with size determined from the X-ray line broadening using equation (3). From the microstructure study it appears that during the initial stage of sintering few hundred nm size grains formed through reaction

among the constituent compounds. At later stage during sintering there is no or negligibly small grain growth. However these grains aggolomerate to form larger grains. Because of the process of aggolomeration the sintering efficiency is less and porosity does not decrease. Percentage porosity of these samples is in the range 7-10.

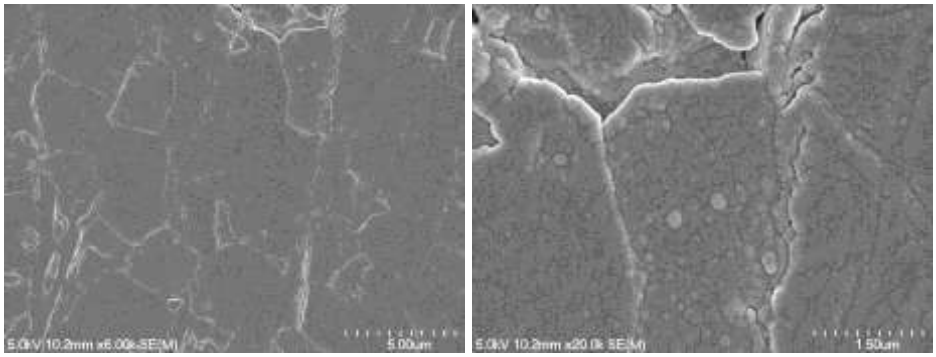

(a) (b)

Figure2: Scanning Electron Micrographs for BTCS1 at different magnifications

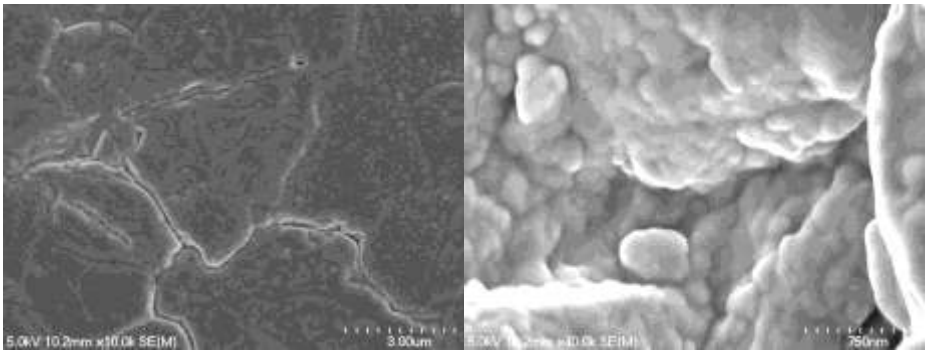

(a) (b)

Figure3: Scanning Electron Micrographs for BTCS3 at different magnifications

CONCLUSION:

Compositions BTS, BTCS1 and BTCS3 are single phase solid solutions having cubic crystal structure. Densification has improved due to Co doping. Scanning Electron Micrographs also show dense microstructure for these compositions.

ACKNOWLEDGEMENTS:

Author is thankful to Prof. Om Parkash and Prof. Devendra Kumar, Department of Ceramic Engineering I.I.T. B.H.U. for extending lab facility to do this work and their valuable guidance.

REFERENCES:

1. Uchino K. Ferroelectrics. Relaxor ferroelectric devices. 1994; 151: 321-330
2. Park SE and Shrout T R. Ultrahigh strain and piezoelectric behavior in relaxor based ferroelectric single crystals. J. Appl. Phys. 1997; 82: 1804-1811
3. Cross LE. Ferroelectrics. Relaxorferroelectrics:An overview. 1994; 151: 305-320
4. Lin JN and Wu TB. Effects of isovalent substitutions on lattice softening and transition character of $BaTiO_3$ solid solutions. J. Appl. Phys. 1990; 68: 985-993
5. Lu SG, Yu ZK, and Chen H. Tunability and relaxor properties of ferroelectric barium stannate titanate ceramics. Appl. Phys. Lett. 2004; 85(22): 5319-5321
6. Mueller V, Beige H, and Abicht HP. Non-Debye dielectric dispersion of barium titanate stannate in the relaxor and diffuse phase-transition state. Appl. Phys.Lett. 2004; 84(8): 1341-1343
7. Geske L, Beige H, Abicht HP et al. Electromechanical Resonance Study of the Diffuse Ferroelectric Phase Transition in $BaTi_{1-x}Sn_xO_3$ Ceramics. Ferroelectrics. 2005; 314: 97-104
8. Shvartsman VV, Kleemann W, Dec J et al. Diffuse phase transition in $BaTi_{1-x}Sn_xO_3$ ceramics: An intermediate state between ferroelectric and relaxor behavior. J. Appl. Phys. 2006; 99: 124111
9. Padilla-Campos L, Diaz-Droguett DE, Lavn R et al. Synthesis and structural analysis of Co-doped $BaTiO_3$ Journal of Molecular Structure. 2015; 1099: 502-509
10. Mansuri A and Mishra A, Structure Evolution of $BaTiO_3$ on Co Doping: X-ray diffraction and Raman study Journal of Physics: Conference Series. 2016; 755: 012018.
11. Stojanovic BD, Foschini CR, and Zaghete MA, Size effect on structure and dielectric properties of Nb-doped barium titanate. J. Mater. Process. Technol. 2003; 143-144:802-806.
12. Mazumdar S and Bhattacharyya GS, Synthesis and characterization of in situ grown magnetoelectric composites in the BaO–TiO–FeO–CoO system. Ceram. Int., 2004; 30: 389-392.
13. Tzing WH, Tuan WH, and Lin HL. The effect of microstructure on the electrical properties of NiO-doped $BaTiO_3$. Ceram.Int. 1999; 25: 425-430.
14. Li T, Li LT., and Zhao JQ. Modulation effect of Mn^{2+} on dielectric properties of $BaTiO_3$-based X7R materials. Mater. Lett. 2000; 44: 1-5.
15. Zhang MS, Yu J, and Chen WH. Optical and structral properties of pure and Ce-doped nanocrystals of barium titanate, Prog. Cryst.Growth Charact. Mater. 2000; 40: 33-42.

16. Chen JF, Shen ZG, and Liu FT. Preparation and properties of barium titanate nanopowder by conventional and high-gravity reactive precipitation methods. Scr. Mater., 2003; 49: 509-514
17. Cheng BL, Button TW, Gabbay M et al. Oxygen Vacancy Relaxation and Domain Wall Hysteresis Motion in Cobalt- Doped Barium Titanate Ceramics. J. Am. Ceram. Soc. 2005; 88: 907-911
18. Wang T, Chen XM, and Zheng XH. Dielectric Characteristics and Tunability of Barium Stannate Titanate Ceramics. Journal of Electroceramics. 2003; 11: 173-178
19. Markovic S, Mitric M, Cvjeticanin N et al. Preparation and properties of $BaTi_{1-x}Sn_xO_3$ multilayered ceramics. Journal of European Ceramic Society. 2007; 27: 505-509
20. Singh S, Singh P, Parkash O et al. Structural and relaxor behavior of $(Ba_{1-x}La_x)(Ti_{0.85}Sn_{0.15})O_3$ ceramics obtained by solid state reaction**.** Journal of Alloys and Compounds. 2010; 493: 522-528
21. Badapanda T, Rout SK, Panigrahi S et al. Phase formation and dielectric study of Bi doped $BaTi_{0.75}Zr_{0.25}O_3$ ceramic. Curr. Appl. Phys. 2009; 9: 727-731
22. Shannon RD. Revised effective ionic radii and systematic studies of interatomic distances in halides and chalcogenides. Acta Cryst. A. 1976; 32: 751-767
23. Kroger FA and Vink HJ, Solid State Physics. Academic Press, New York; 1956.